On reduced models to approximate particle beams and plasma physics problems

FRANCK ASSOUS
Ariel University Center
Department of Computer Sciences and Mathematics
Ariel 44837
ISRAEL
franckassous@netscape.net

Abstract: This paper is devoted to the construction of models to approximate particle beams and plasma physics problems. In recent years, solving numerically problems which couple charged particle to electromagnetic fields has given rise to challenging mathematical and scientific computing developments. In the industry, a variety of examples can be thought of, such as the ion or electron injectors for particle accelerators, the free electron lasers, the hyperfrequency devices, the vulnerability of spatial devices to particle flows, etc. The mathematical model which is most relevant in describing the physics of such problems is provided by the time-dependent coupled Vlasov-Maxwell system of equations. Eventhough this model is necessary in a number of cases, it leads to very expensive computations and simpler, i.e *reduced models* are required. The main lines of this paper will treat about the analysis and the development of the reduced models. We present two situations in which this strategy can be applied. Numerical results illustrate the possibilites of the approach.

Key–Words: Vlasov-Maxwell, Vlasov-Poisson, paraxial approximation, reduced models, PIC code

1 Introduction

Charged particles appear essentially in two kinds of physics problems: charged particle beams, like in hyperfrequency devices or vacuum diode technology, and plasma physics, a plasma being roughly speaking a gas of quasi neutral charged particles. Plasmas are involved in a lot of real-life applications. They are commonly used in Science and Technology and play an important role in the energy production (for instance in the magnetic confinement fusion). They are also ingredients of instruments and others devices (see the Introduction of [16] for a survey of the applications). Moreover, all fusion applications involve non linear interaction of charge particle beams. As a consequence, there is a need in finding mathematical models which can be used for numerical simulations.

Quite complete mathematical models to solve these problems are based on the time-dependent Vlasov-Maxwell system of equations, sometimes under the relativistic assumption. Indeed, there exists a strong correlation between the Maxwell equations and models that describe the motion of particles. This correlation is at the origin of most of the coupled models, where the Maxwell equations (or any kind of equations approximating them) appear in parallel with (and depending on) other models of equations.

However, the numerical solution of the Vlasov-Maxwell system requires an important computational effort, and can be very expensive in terms of computational cost. This point is particularly important if the code has to be intensively used to analyse a lot of experimental results. In such a situation, one have to take into account the particularities of the physical problem (geometries, physical properties, etc.) to derive *reduced* models leading to cheaper computations.

Deriving such realistic but rigourous mathematical models is challenging. Moreover, efficient algorithms are needed for instance in order to be able to select between several issues in the design of devices, especially to take into account the three-dimensional effects.

In this paper, we propose two examples of such problems, for which reduced models have been derived leading to easier computations than the original model. The outline of the paper is as follows. In the next Section, we recall the Vlasov-Maxwell system of equations, and the methods generally used to solve it. In Section 3, we introduce two examples of reduced models. The first is based on a low frequency assumption, whereas the second is derived from a paraxial hy-

pothesis. Numerical applications illustrate the possibilities of this approach. Concluding remarks follow.

2 The Vlasov-Maxwell model

In this section, we recall the Vlasov-Maxwell system of equations and briefly review the most popular methods to solve it.

2.1 The Vlasov equation

Let us consider a population of charged particles, with a mass m and a charge q, submitted to the electromagnetic Lorentz force

$$\mathbf{F} = q\left(\mathcal{E}(\mathbf{x}, t) + \mathbf{v}(t) \times \mathcal{B}(\mathbf{x}, t)\right), \tag{1}$$

that describes how the electromagnetic field $\mathcal{E}(\mathbf{x}, t)$ and $\mathcal{B}(\mathbf{x}, t)$ acts on a particle with a velocity $\mathbf{v}(t)$. Each particle is characterized by its position $\mathbf{x}$ and its velocity $\mathbf{v}$ in the so-called phase space $(\mathbf{x}, \mathbf{v})$. We introduce the distribution function $f(\mathbf{x}, \mathbf{v}, t)$, which can be defined as the average number of particles in a volume $d\mathbf{x}d\mathbf{v}$ of the phase space. Assuming that collisions between particles can be neglected, the distribution function $f(\mathbf{x}, \mathbf{v}, t)$ is solution to the following transport equation, named the Vlasov equation

$$\frac{\partial f}{\partial t} + \mathbf{v} \cdot \nabla_{\mathbf{x}} f + \frac{q}{m}(\mathcal{E}(\mathbf{x}, t) + \mathbf{v} \times \mathcal{B}(\mathbf{x}, t)) \cdot \nabla_{\mathbf{v}} f = 0. \tag{2}$$

Remark 2.1 *If collisions are not neglected, they induce changes in the particle velocity. To model these collisions, one usually introduces the collision operator $Q(f)$, that can be linear, quadratic, etc., depending on the physics involved. The mathematical tools as well as the numerical methods involved in that case are fairly different from these we intend to use, and then, handle the collisions is excluded from this research proposal.*

For the relativistic case, denote by $\mathbf{p}$ the momentum and c the speed of the light, we introduce the distribution function $f(\mathbf{x}, \mathbf{p}, t)$ such that

$$\mathbf{p} = \gamma m \mathbf{v}, \quad \text{with} \quad \gamma m = \frac{\sqrt{|\mathbf{p}|^2 + m^2 c^2}}{c},$$

then the relativistic Vlasov equation is obtained by substituting the term $\frac{1}{m}\nabla_{\mathbf{v}} f$ in Equation (2) by the term $\nabla_{\mathbf{p}} f$.

Solving the time-dependent Vlasov equation in the six-dimensional phase space $(\mathbf{x}, \mathbf{p})$ (or $(\mathbf{x}, \mathbf{v})$ in a non-relativistic case) with a grid method (finite difference, finite volume or finite element method) is almost impossible, since we rapidly reach the limit in memory available on a computer, leading then to an intractable cpu time. For this reason, a well suited method is the widely used particle method (see [5] or [20] for a theoretical description). However, due to the increase of the computer memory, especially when using supercomputer or multiple processors (parallel computers), grid methods are considered again for one or two-dimensional Vlasov problems coupled with the static Poisson equation.

Solving the Vlasov equation by means of a particle method consists in approximating the distribution function $f(\mathbf{x}, \mathbf{v}, t)$ at any time t, by a linear combination of delta distributions in the phase space:

$$f(\mathbf{x}, \mathbf{v}, t) \simeq \sum_k w_k \, \delta(\mathbf{x} - \mathbf{x}_k(t))\delta(\mathbf{v} - \mathbf{v}_k(t)) \, , \tag{3}$$

where each term of the sum can be identified with a macro-particle, characterized by its weight w_k, its position $\mathbf{x}_k$ and its velocity $\mathbf{v}_k$. This distribution function is a solution of the Vlasov equation (2) if and only if $(\mathbf{x}_k, \mathbf{v}_k)$ is a solution to the differential system:

$$\frac{d\mathbf{x}_k}{dt} = \mathbf{v}_k \, , \tag{4}$$

$$\frac{d\mathbf{p}_k}{dt} = \mathbf{F}(\mathbf{x}_k, \mathbf{p}_k) \, , \tag{5}$$

which describes the time evolution of a particle k, submitted to the electromagnetic Lorentz force $\mathbf{F}$ (see (1)). This system is generally solved by an explicit time discretization scheme. A leapfrog scheme is well-adapted in this case (see [3] for more details).

2.2 The Maxwell equations

The expressions of the charge and the current density induced by the motion of these particles are given by

$$\rho(\mathbf{x}, t) = q \int_{\mathbb{R}_v^3} f(\mathbf{x}, \mathbf{v}, t) \, d\mathbf{p}, \tag{6}$$

$$\mathcal{J}(\mathbf{x}, t) = q \int_{\mathbb{R}_v^3} f(\mathbf{x}, \mathbf{v}, t) \, \mathbf{v} \, d\mathbf{p}, \tag{7}$$

that express the coupling of the Maxwell and Vlasov equations. Indeed $\rho(\mathbf{x}, t)$ and $\mathcal{J}(\mathbf{x}, t)$ appear as the right-hand sides of the Maxwell equations (in the vacuum)

$$\frac{1}{c^2}\frac{\partial \mathcal{E}}{\partial t} - \nabla \times \mathcal{B} = -\mu_0 \mathcal{J} \, , \tag{8}$$

$$\frac{\partial \mathcal{B}}{\partial t} + \nabla \times \mathcal{E} = 0 \, , \tag{9}$$

$$\nabla \cdot \mathcal{E} = \frac{\rho}{\varepsilon_0} \, , \tag{10}$$

$$\nabla \cdot \mathcal{B} = 0 \, , \tag{11}$$

where the constants ε_0, μ_0 are respectively the dielectric permittivity and the magnetic permeability in the vacuum, that satisfies $\varepsilon_0 \mu_0 c^2 = 1$.

The Vlasov and Maxwell equations *separately* are linear hyperbolic systems, but the expression of the Lorentz force $\mathbf{F}$ in a way and those of the charge and current density ρ and $\mathcal{J}$ in another way leads to a strong coupling, that makes the whole problem quadratic. Indeed, the term

$$\mathbf{F} \cdot \nabla_{\mathbf{p}} f = q(\mathcal{E}(\mathbf{x}, t) + \mathbf{v} \times \mathcal{B}(\mathbf{x}, t)) \cdot \nabla_{\mathbf{p}} f$$

is a quadratic term since $\mathcal{E}$ and $\mathcal{B}$ depend on the distribution function f in an affine way, through ρ and $\mathcal{J}$.

For computing the solution of Maxwell's equations, some of the numerical codes which are developed are based on finite difference approximations of Maxwell's equations on structured meshes. These are completely explicit, at least when the charge conservation equation $\partial_t \rho + \nabla \cdot \mathcal{J} = 0$ is numerically verified. The first and probably most popular method was introduced by Yee [24] in 1966, and is straightforward to implement in simple cases. However, despite its simplicity and its efficiency, as soon as the domain geometry becomes too complex, or when local refinements are necessary, the structured mesh strategy is not well adapted, and suffers from the inaccurate representation of the solution on curved boundaries.

An alternative is to use the flexibility of unstructured meshes to approximate complex geometries and to achieve local refinements. For the finite element discretization, different formulations are available. Examples are the edge elements [19], the vector finite element method [22], or the Cartesian elements eventually in a constrained form [2] . Other nodal finite element techniques based on a least-squares approach were also proposed. Concerning finite volumes solvers, several kind have been developed : Delaunay-Voronoi finite volume methods [17], or other types of methods include traditional vertex centered or cell centered [18] finite volume methods, regarding the Maxwell equations as a first-order strictly hyperbolic system.

From a mathematical point of view, the Cauchy problem for the Vlasov-Maxwell sytem is quite well understood. The existence of a weak solution was proved by DiPerna-Lions [8]. For the Vlasov-Maxwell system with boundary conditions, see [13]. We also refer to [6] and [9] for a survey on the existence of weak solutions. For the classical solutions, Glassey et. al [11], [12] have shown that the existence of a global solution depends only on the control of high velocities. The local in time existence and uniqueness of strong solutions was proved by Degond [7].

From a numerical point of view, this model is very complete but also not easy to solve numerically, in particular in a three-dimensional domain. Evenhougth this is necessary in several cases (see [2], [3]), one easy understands the need of deriving simpler (but accurate) models, by exploiting given physical assumptions. Hence, in some cases, assuming that the problem is static allows to replaced Maxwell's equations by a *reduced model* like Poisson's equation. Following this idea, one can obtain a hierarchy of reduced models, like Vlasov-Poisson, Vlasov-Darwin, paraxial models, gyrokinetic models, laser-plasma interaction models, etc...generally obtained by exploiting specific geometries/properties of the problem. Often, these models have been derived by physicists in a formal way. We think there is a need first to justify them, then to precise how much accurate they are, finally to improve their accuracy. An important part is also to obtain by these techniques new approximate models, and to develop new algorithms. To our opinion, this will be a significant progress for improving the comprehension of complex problems.

In what follows, taking into account the particularities of the physical problems, we derive two such reduced models leading to cheaper computations.

3 A low frequency reduced model

As a first example of reduced model, we consider the modelling and the simulation of the multipaction effect. This is an unwanted breakdown phenomenon, wich can occur in high power space components. This can be schematized as follows: consider for instance in a step waveguide (see Fig. 1) a free electron accelerated by an applied electromagnetic field. A secondary emission and the electron reflection result from the electron impact on the waveguide wall. These two electrons may now be accelerated across the waveguide if the applied field reverses at the proper time, and strike an opposite waveguide wall leading to new secondary and reflected electrons. This process repeated many times can lead to an exponential growth of the charge density. In this case the component can no more fulfill its function and may even be destroyed. Obviously, this multipaction process can occur under some conditions on the cycles of the

applied field (to accelarate the electrons) and on the energy of the incident electrons (to induce the number of particles to increase). The aim of the modelling is to determine, for a given waveguide and an applied field, a threshold voltage above which multipaction can occur. This quantity depends first on the component parameters (the wall material, the profile of the component, etc.), and also on the experimental conditions, essentially the single or multicarrier analysis: in the first case, the multipaction occurs when the magnitude of the voltage is and remains at a constant level above the multipaction threshold. In the second case, the multipaction occurs every time that the peak voltage, obtained by combining all the carriers in phase, is above the multipaction threshold. Therefore simulations of this phenomenon require *a priori* a Maxwell-Vlasov solver.
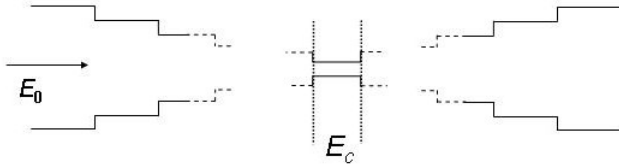

Figure 1: step waveguide.

3.1 From Vlasov-Maxwell to Vlasov-Poisson

By using first the linearity of the Maxwell equations, one can decompose the electric field $\mathcal{E}$ into two parts, $\mathcal{E} = \mathcal{E}_{\text{ext}} + \mathcal{E}_{\text{s}}$, where $\mathcal{E}_{\text{ext}}$ is the applied field which is external, and $\mathcal{E}_{\text{s}}$ denotes the self-consistent field, created by the electrons displacement. Remark then that the external field is solution to the time-dependent Maxwell equations, without any coupling with the Vlasov equation. For the self-consistent field $\mathcal{E}_{\text{s}}$, using that the velocity of the extracted electrons $\mathbf{v}_{\text{ele}}$ is very small compared to the light velocity of the electromagnetic waves, one introduces a small parameter $\varepsilon = \dfrac{\mathbf{v}_{\text{ele}}}{c}$. Following [21], reduced models of Maxwell's equations can be derived after a scaling and an asymptotic expansion of the solution in power of this parameter ε. There, it is proved that the quasi-static Vlasov-Poisson model is a first order approximation of the Vlasov-Maxwell equations. Hence, one assume that $\mathcal{E}_{\text{s}}$ can be accurately computed by solving the Poisson problem

$$-\Delta\phi = \frac{\rho(t)}{\varepsilon_0} \text{ with } \mathcal{E}_{\text{s}} = -\nabla\phi , \qquad (12)$$

coupled with the Vlasov equation, and supplemented with suitable boundary and initial conditions. The main advantage of this model is that Equation (12) is not explicitly time dependent, the density $\rho(t)$ being given at each timestep of the Vlasov equation solution. This avoids to use a time stepping method for the self-consistent field, that is generally expensive in terms of computing time.

Based on the above remarks, the methodology for the numerical study of the multipaction effect can be divided into three steps.

1. **Computation of the overvoltage coefficient:** the propagation of an ingoing plane wave of amplitude E_0 is computed with a time dependent Maxwell solver to obtain the amplitude E_c of the wave in the gap (see Fig. 1). Then, the overvoltage coefficient η is determined with

$$\eta = \frac{|E_c|}{|E_0|} . \qquad (12)$$

Since the coefficient η depends only on the geometry of the waveguide and on the frequency of the ingoing wave, the computations are carried out only once for each applied frequency.

2. **Solving Vlasov-Poisson in a reduced domain:** Consider a given exterior field of the form

$$E(t) = E \sum_{i=1}^{i=n} \cos(2\pi f_i t) . \qquad (13)$$

As $n = 1$ (resp $n > 1$), it is a single carrier (resp. multicarrier) simulation. In the computational domain restricted to the gap area, solve the Vlasov-Poisson equations augmented with secondary emission laws to model the behaviour of the extracted electrons (cf. [1]). From these results, one deduces the multipaction threshold voltage.

3. **Determination of the mutipaction threshold:** from the amplitude E used in the step 2 and the values η of the step 1, on can easily deduce the amplitude E_0 at the input of the component corresponding to the multipaction threshold. Its power is given by

$$P_0 = \sqrt{\frac{\omega^2}{c^2} - \frac{\pi^2}{L^2}} \frac{HL}{2\mu_0\omega} E_0^2 ,$$

where H and L denote the height and the transverse dimension of the waveguide.

Remark 3.1 *The secondary emission laws used here are essentially from [23] and [10]. We refer the interested reader to these references for details. Let us briefly recall some principles. The data needed to fully describe the emitted electrons are the yield as a function of the incident electron energy and angle with respect to the normal, and the energy and angular distribution of the emitted electrons. The total yield is conventionally divided into two groups of electrons according to their emission energy. The reason for separating the yield into two parts is that these quantities depend in different ways on the incident electron energy and angle. In all these secondary emission laws, two particles (the reflected and the secondary) are created for each incident one, with or without any multipaction effect. When there is no multipaction, the number of particles grows each of them carries a smaller weight, so that the total charge decreases.*

3.2 Numerical illustration

Let us consider the two-dimensional domain depicted in Fig. 1. The ingoing signal is a sum of three given frequencies: $f_1 = 10.911$ GHz, $f_2 = 11.075$ GHz and $f_3 = 11.158$ GHz. The corresponding overvoltage coefficients we obtain are $\eta_1 = 9$, $\eta_2 = 9.1$ and $\eta_3 = 9.2$. The second step is a Vlasov-Poisson simulation in the gap area. The avalanche of electrons occurs when the envelope of the applied voltage in this gap area becomes greater than the multipaction threshold. In such a multicarrier multipaction, the envelope of the applied voltage is obtained by combining all the carriers in phase. In this case, the multipaction effect is characterized by a periodic series of charge density peaks corresponding to the voltage of the envelope. In the numerical simulations, the charge grows exponentially as a multipaction occurs during an envelope peak, but decays again when the voltage falls below the threshold. In order to model the presence of particles in the component, we have to inject them with a well adapted numerical procedure. In a multicarrier simulation, it is sufficient to seed the component at regular time intervals. Examples are shown on Fig. 2 and 3.

Remark 3.2 *In a single carrier simulation, the threshold is characterized by the exponentially growing charge density. In practice, one considers that the threshold is reached as the particle density is about $10^2 - 10^3$ particles/m^3. This corresponds to a threshold voltage error of approximatively 1 V. Another difference with a multicarrier simulation is also on the particle injection procedure. It is more efficient now to seed the component at the initial time of the simulation.*
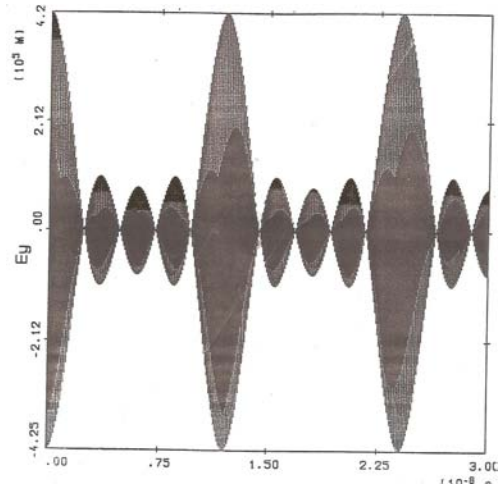

Figure 2: E_y component.

4 A highly relativistic reduced model

This second example is devoted to the case of high energy short beams. The aim is to study the transport of a bunch of highly relativistic charged particles in the interior of a perfectly conducting tube. Following [15], one can derive a reduced model which exploits the property that the particles of the beam remain close to an optical axis.

4.1 From Vlasov-Maxwell to a paraxial model

Consider a beam of charged particles which moves in the interior of a perfectly conducting hollow tube. We choose the axis of the tube as the $z-$axis. Assuming that the beam is a high energy short beam, Laval et al. [15] have derived a reduced model in the following way. The high energy assumption means that relativistic factor $\gamma >> 1$. Consequently, since the particle velocity $\mathbf{v}$ is close to c for any particle in the beam, one rewrites the Vlasov-Maxwell equations in the beam frame, which moves along the z-axis with the light velocity c. Hence, we set

$$\zeta = ct - v_z, \quad v_\zeta = c - v_z.$$

According to [15], it is worthwhile to distinguish the transverse quantities (denoted by $\perp$) from the longitudinal ones. For the position and the velocity, we introduce

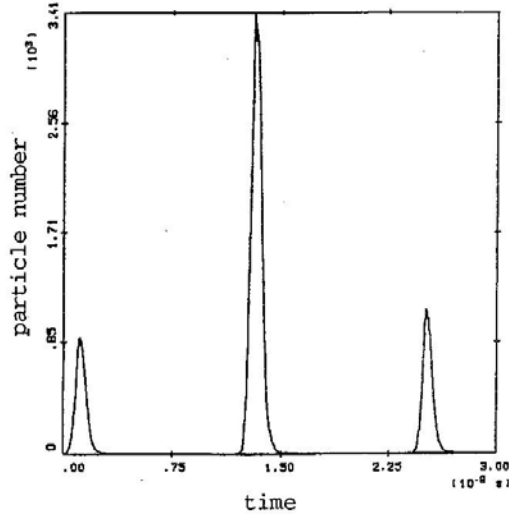$$\mathbf{x}_\perp = (x, y), \quad \mathbf{v}_\perp = (v_x, v_y).$$

Figure 3: particle number.

For the differential operartors (φ is a scalar funtion)

$$\mathbf{grad}_\perp \varphi = (\frac{\partial \varphi}{\partial x}, \frac{\partial \varphi}{\partial y}), \quad \mathbf{curl}_\perp \varphi = (\frac{\partial \varphi}{\partial y}, -\frac{\partial \varphi}{\partial x}),$$

and for a transverse vector field $\mathbf{A}_\perp = (A_x, A_y)$,

$$\mathrm{div}_\perp \mathbf{A}_\perp = \frac{\partial A_x}{\partial x} + \frac{\partial A_y}{\partial y},$$

$$curl_\perp A = \frac{\partial A_y}{\partial x} - \frac{\partial A_x}{\partial y},$$

$$div_{\mathbf{v}_\perp} A = \frac{\partial A_x}{\partial v_x} + \frac{\partial A_y}{\partial v_y}.$$

With the above notations, Vlasov equation (2) in the beam frame can be written

$$\frac{\partial f}{\partial t} + \mathbf{v}_\perp \cdot \mathbf{grad}_\perp f + v_\zeta \frac{\partial f}{\partial \zeta} +$$

$$+ div_{\mathbf{v}_\perp}[\frac{1}{\gamma m}((\mathbf{I} - \frac{1}{c^2}\mathbf{v} \otimes \mathbf{v}) \cdot \mathbf{F}_\perp - \frac{1}{c}(1 - \frac{v_\zeta}{c})\mathbf{v}_\perp F_z)f] +$$

$$\frac{\partial}{\partial v_\zeta}[\frac{1}{\gamma m c}((1 - \frac{v_\zeta}{c})\mathbf{v}_\perp \cdot \mathbf{F}_\perp + (2 - \frac{v_\zeta}{c})v_\zeta F_z)f) = 0,$$

where

$$\gamma = (2v_\zeta/c - 1/c^2(\mathbf{v}_\perp^2 + v_\zeta^2))^{-1/2}.$$

Next, Ampere and Poisson equations (8-10) give

$$\frac{1}{c^2}\frac{\partial \mathcal{E}_\perp}{\partial t} - \mathbf{curl}_\perp \mathcal{B}_z + \frac{1}{c}\frac{\partial \mathcal{K}_\perp}{\partial \zeta} = -\mu_0 \mathcal{J}_\perp, \tag{13}$$

$$\frac{1}{c^2}\frac{\partial \mathcal{E}_z}{\partial t} + \frac{1}{c}\mathrm{div}_\perp \mathcal{K}_\perp = -\mu_0 \mathcal{J}_\zeta, \tag{14}$$

$$\mathrm{div}_\perp \mathcal{E}_\perp - \frac{\partial \mathcal{E}_z}{\partial \zeta} = \frac{1}{\epsilon_0}\rho, \tag{15}$$

with $\mathcal{K}_\perp = (\mathcal{K}_x = \mathcal{E}_x - c\mathcal{B}_y, \mathcal{K}_y = \mathcal{E}_y + c\mathcal{B}_x)$, and $\mathcal{J}_\zeta = \rho c - \mathcal{J}_z$.

Similarly, equations (9-11) are equivalently written in the beam frame as

$$\frac{\partial \mathcal{B}_\perp}{\partial t} + \mathbf{curl}_\perp \mathcal{E}_z + \frac{\partial}{\partial \zeta}(\mathcal{E}_\perp \times \mathbf{e}_z) = 0, \tag{16}$$

$$\frac{\partial \mathcal{B}_z}{\partial t} + curl_\perp \mathcal{K}_\perp = 0, \tag{17}$$

$$\mathrm{div}_\perp \mathcal{B}_\perp - \frac{\partial \mathcal{B}_z}{\partial \zeta} = 0, \tag{18}$$

whereas the electromagnetic force $\mathbf{F}$ becomes

$$\mathbf{F}_\perp = q(\mathcal{K}_\perp + \mathbf{v}_\perp \times \mathbf{e}_z)B_z + \mathbf{v}_\zeta(\mathcal{B}_\perp \times \mathbf{e}_z),$$

$$\mathbf{F}_z = q(\mathcal{E}_z + \mathbf{v}_\perp \cdot (\mathcal{B}_\perp \times \mathbf{e}_z)).$$

The treatment of the boundary conditions can be handled in the same way. We refer the reader to [15] for details.

Now, to derive a paraxial model, one then introduces a scaling of the equations. The central assumptions are

- First exploiting the short beams assumption, i.e. the dimensions of the beam are small compared to the longitudinal length of the device.

- Moreover, one assumes that the longitudinal particle velocities v_z are close to the light velocity c.

- Finally, the transverse particle velocities are small compared to c.

Hence one introduces the transverse characteristic velocity of the particles $\overline{v}$, and define a small parameter η, $\eta = \frac{\overline{v}}{c} \ll 1$.

Using that the particle velocities are close to c, we conclude that v_ζ is of the order $\overline{v}^2/c$ and one choose

$$\overline{w} = \eta^2 c \tag{19}$$

as a characteristic longitudinal velocity of the particles in the beam frame. Finally, the characteristic time can be taken as $T = l/\overline{v}$, where l denotes the characteristic dimension of the beam. Then, defining dimensionless independent variables, one thus obtains a Vlasov-Maxwell system of equations expressed in dimensionless variables, where appear powers of the small parameter η.

The next step consists in developing asymptotic expansions of all these quantitites ($f, \mathcal{E}, \mathcal{B}, \mathbf{F}$, etc.) in

powers of the small parameter η, as

$$f = f^0 + \eta f^1 + ...,$$
$$\mathcal{E} = \mathcal{E}^0 + \eta \mathcal{E}^1 + ...,$$
$$\mathbf{F} = \mathbf{F}^0 + \eta \mathbf{F}^1 + ...$$

It is proved in [15] that the resulting paraxial model, obtained by retaining the first four terms in the asymptotic expansion, is an approximation exact up to the order 3 in η.

In this paper, we consider the axisymmetric counterpart. Using the coordinates (r, θ, ζ) (with obvious notations), the electric field is now denoted (E_r, E_θ, E_z), the magnetic one (B_r, B_θ, B_z). One thus obtains that the electromagnetic force $\mathbf{F}$ is entirely determined by the transverse fields, which are zero order fields, the longitudinal ones, that are first order fields, and the so-called pseudo-fields $\mathcal{E}_r = E_r - cB_\theta$ and $\mathcal{E}_\theta = E_\theta + cB_r$, which are second order corrections. Hence, the paraxial model of ultra-relativistic Maxwell equations is written:
For the zero order fields:

$$\begin{cases} E_r = cB_\theta = \dfrac{1}{\varepsilon_0\, r} \int_0^r \rho s\, ds \\[4mm] E_\theta = B_r = 0 \end{cases} \quad (20)$$

For the first order fields:

$$\begin{cases} \dfrac{\partial E_z}{\partial r} = \dfrac{\partial B_\theta}{\partial t} \\[4mm] E_z(r = R) = 0 \end{cases} \text{ and } \begin{cases} \dfrac{\partial B_z}{\partial r} = \mu_0 J_\theta \\[4mm] \int_0^R B_z r\, dr = 0 \end{cases} \quad (21)$$

For the second order pseudo-fields $\mathcal{K}_r$ and $\mathcal{K}_\theta$:

$$\begin{cases} \mathcal{K}_r = \dfrac{1}{r} \int_0^r (\mu_0 c J_\zeta - \dfrac{1}{c}\dfrac{\partial E_z}{\partial t}) s\, ds \\[4mm] \mathcal{K}_\theta = -\dfrac{1}{r} \int_0^r \dfrac{\partial B_z}{\partial t} s\, ds, \end{cases} \quad (22)$$

where J_ζ is defined by $J_\zeta = \rho c - J_z = q \int v_\zeta f d\mathbf{v}$.

We approximate these equations with specific numerical schemes based on a finite-difference approach. The order of the computations is induced by the asymptotic expansion. Hence, the zero order fields E_r, B_θ have to be first computed, and are necessary to obtain the first order quantities E_z. Similarly, the computation of the second order pseudo-fields $\mathcal{K}_r$ and $\mathcal{K}_\theta$ requires the first order approximate fields E_z and B_z. Note that the longitudinal magnetic component B_z only depends on the azimuthal current density

J_θ. In particular, B_z is identically zero as soon as J_θ vanishes.

As we are working in the beam frame, the particles drift slowly in the direction $\zeta > 0$. As a consequence, the computational domain is defined as a simple rectangular domain in variables (r, ζ), $0 \le r \le R$, $0 \le \zeta \le Z$. The value of R is given by the radius of the cylindrical tube, and Z is chosen in such a way that the particles remain in a fixed geometrical domain $\Omega \times]0, Z[$ (in the beam frame), during the time interval $[0, T]$ of the simulation.

As an example, we give here the numerical scheme for E_r (or equivalently B_θ). For a given or computed charge density, equation (20) can be solved by simple numerical integration methods. For instance, consider a classical 2-point Newton-Cotes formula, which is exact for the first-order degree polynoms. We thus obtain for E_r^{n+1} (the same for B_θ^{n+1})

$$E_{r,i,j}^{n+1} = \frac{1}{r_i \varepsilon_0} \frac{\Delta r}{2} [\rho_{1,j}^{n+1} r_1 + 2\rho_{2,j}^{n+1} r_2 + ... + \rho_{i,j}^{n+1} r_i] \quad (23)$$

Similar numerical schemes can be derived for the other components. More details can be found in [4].

4.2 A numerical example

As we are working in the beam frame, the computational domain is the rectangle $]0, R[\times]0, Z[$ in variables (r, ζ). The mesh sizes $\Delta r, \Delta \zeta$ are chosen such that $R/\Delta r = Z/\Delta \zeta = 0.01$. The time step Δt is taken in order to comply with the CFL stability condition. As a numerical example, consider a bunch of particles emitted with velocities such that the paraxial assumptions are verified. According to stability condition [5], more than 10 particles are placed in each cell, with the same weight and a charge following

$$w = \frac{\mathbf{J}\Delta t}{Ne},$$

where $\mathbf{J}$ is the total current to be emitted, and N the particle number. Fig. 4 and 5 show respectively the self-consistent electric radial and longitudinal field E_r, E_z obtained after 50 time steps of simulation with the resulting PIC paraxial code. The corresponding charge density ρ, computed with the Vlasov part of the code, is depicted on Fig. 6.

From a physical point of view this problem can be compared with the following "analytical" problem. Consider the same problem where the charge and current densities $(\rho, \mathbf{J})$ are known functions which verify

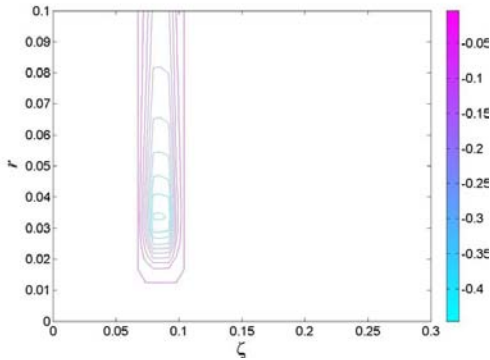$$r\rho(r, \zeta, t) = qwK(r, \zeta - vt),$$
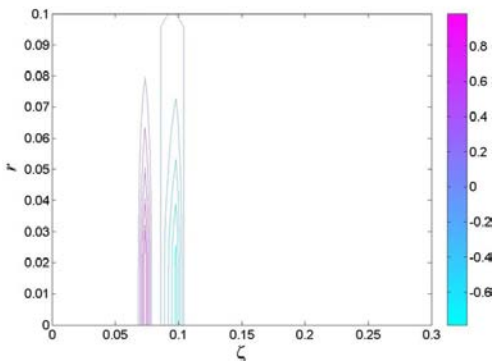
Figure 4: E_r component (50 Δt).

Figure 5: E_z component (50 Δt).

Figure 6: charge density ρ (50 Δt).

Figure 7: E_r component, hypothetical Vlasov solver.

and

$$rJ_\theta(\zeta, t) = -qw/\upsilon K(r, \zeta - \upsilon t)\,,$$
$$rJ_\zeta(\zeta, t) = qw\upsilon K(r, \zeta - \upsilon t)\,.$$

Above $K(r, \zeta)$ is a given piecewise linear continuous function, constant for $\zeta \in [b_1, b_2]$, and equal to zero outside $[a_1, a_2]$ (with $0 < a_1 < b_1 < b_2 < a_2 < Z$. This case is of interest, because an analytic expression of the solutions can be easily calculated. Moreover, υ is a given drift velocity along the ζ-axis, chosen to design a hypothetical Vlasov solver. This problem exhibits a behavior close to the real Vlasov solver. As an example, result for the E_r component is shown on Fig. 7. One can observe a good agreement between the real and the hypothetical Vlasov solver. The difference observed is a direct consequence of coupling between finite-difference methods and particle-in-cell ones. Interaction between particles causes the shape to be more complicated than a simple flat "hat" as in the hypothetical Vlasov example.

5 Conclusion

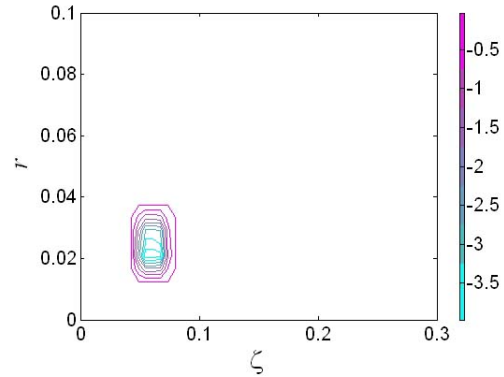In this paper, we are concerned with the development of numerical methods required for solving particle beams and plasma physics problems. Exploiting the particularities of the physical problem, we proposed to develop reduced models. We hope this approach to be very powerfull in its ability to get accurate, but fast and easy to implement algorithms. As a first example we proposed a numerical methodology to study the multipaction effect, that significantly improved the computational time of the simulations. In the second example, a PIC method for solving a paraxial model of highly relativistic beam has been developed. Numerical results were presented to illustrate the possibilities these models.

References:

[1] F. Assous, V. Courtonne, C. Quine, J. Segré, Numerical simulations versus experimental measurements of the multipaction effect, *WIT Trans. Modelling and Simulation*, Vol. 17, 673-684,1997.

[2] F. Assous, P. Degond, E. Heintzé, P.A. Raviart and J. Segré, On a finite element method for solving the three dimensional Maxwell equations, *J. Comput. Physics*, 109(2), 1993, 222-237.

[3] F. Assous, P. Degond, and J. Segré, A particle-tracking method for the 3D electromagnetic PIC codes on unstructured meshes, *Comp. Phys. Com.*, **72**, 105–114, 1992.

[4] F. Assous, F, Tsipis, Numerical paraxial approximation for highly relativistic beams, 14th IASTED conference on Applied Simulation and Modelling, M.H. Hamza Ed., 100–105, Rhodes, Greece, 2006.

[5] C.K. Birdsall and A.B. Langdon, *Plasmas Physics via Computer Simulation* (New York: Mac.Graw-Hill, 1985).

[6] F. Bouchut, F. Golse, M. Pulivrenti, *Kinetic Equations and Asymptotic Theory* Gauthiers-Villars series in Applied Mathematics (2000).

[7] P. Degond, Local existence of the solution of the Vlasov-Maxwell equations and convergence to the Vlasov-Poisson equations for infinite high velocity, *Math. Meth. Appl. Sci.* 8(4), 533-558 (1986).

[8] R. J. DiPerna, P.L. Lions, Global weak solutions of Vlasov-Maxwell system *Commun. Pure Appl. Math.*, 42(6):729-757,1989.

[9] R. J. DiPerna, P.L. Lions, Global weak solution of kinetic equations *Rend. Sem. Math. Univ. Politec. Tonino*, 46, 259-288, 1998.

[10] Galan, L., Pietro, P., Morant, C., Soriano, L. & Rueda, F. Study of secondary emission properties of materials for high RF power in space, *final report for ESTEC contract No. A0 6577*, 1990.

[11] R. Glassey, The Cauchy problem in kinetic theory. SIAM, Philadelphia, 1996.

[12] R. Glassey, W. Strauss W, Singularity formation in a collisionless plasma could only occur at high velocities. *Arch. Rat. Mech. Anal.*, 92, 56-90, (1986).

[13] Y. Guo, Global weak solutions of Vlasov-Maxwell system with boundary conditions, *Commun. Math. Phys.*, 154(2):245-263,1993.

[14] R.W. Hockney and J.W. Eastwood, *Computer Simulation Using Particles* (McGraw-Hill, New York, 1981).

[15] Laval, G., Mas-Gallic and S., Raviart, P. A.: Paraxial approximation of ultrarelativistic intense beams. Numer. Math. **69(1)**, 33-60, 1994.

[16] J.D. Lawson, *The Physics of Charged-Particle Beams*, Clarendon Press, Oxford, 1988.

[17] N.K. Madsen and R.W. Ziolkowski, Numerical solution of Maxwell's equations in the time domain using irregular nonorthogonal grids, *Wave Motion*, **10**, 583–596, 1988.

[18] C.-D. Munz, P. Omnes, R. Schneider, A three-dimensional finite volume solver for the Maxwell equations with divergence cleaning on unstructured meshes, *Comp. Phys. Com.*, **130 (1-2)**, 83–117, 2000.

[19] J.C. Nédélec, Mixed finite elements in $\mathbb{R}^3$, *Numer Math.*, **35**, 315–341, 1980.

[20] P.A. Raviart, *An Analysis of Particle Methods* (Springer Verlag, Berlin, 1985).

[21] P.A. Raviart, E. Sonnendrücker, Approximate models for the Maxwell equations, *J. Comput. Appl. Math.*, **63**, 69–81, 1995.

[22] G. Rodrigue, D. White , A vector finite element time-domain method for solving Maxwell's equations on unstructured hexahedral grids, *SIAM J. Sci. Comput.*, **23**, 683–706, 2001.

[23] Schou, J. Secondary electron emission from solids by electron and proton bombardment, *Scanning Microscopy*, 1988, **2**,607-632.

[24] K.S. Yee, Numerical solution of initial boundary value problems involving Maxwell's equations in isotropic media, *IEEE Trans. Antennas and Propag.*, **14**, 302–307, 1966.